

En este número de la revista la sección DE ANIVERSARIO está dedicada al tema de "Química de frontera". Hemos pedido a varios científicos nacionales y extranjeros que nos escriban un artículo de divulgación sobre un tópico relacionado con su tema de investigación. Para empezar tenemos éste, escrito por Jean-Luc Brédas, actualmente en el Instituto de Tecnología de Georgia, que resalta la importancia de los procesos de transferencia electrónica y de transferencia energética en materiales  $\pi$ -conjugados, que es el tema con el que se otorgó el premio Nobel de Química el año 2000. ¡Que los lectores disfruten esta "Química de frontera"!

## Electro-active $\pi$ -Conjugated Oligomers and Polymers: A Molecular Picture of Charge-Transfer Processes

*J.L. Brédas, D. Beljonne, V. Coropceanu, and J. Cornil\**

### I. Introduction

Inorganic semiconductor devices such as transistors have been instrumental in shaping the development of our society of information and communication. Recently, the electronics and photonics technologies have opened their materials base to organics, in particular  $\pi$ -conjugated oligomers and polymers. The goal with organics-based devices is not necessarily to attain or exceed the level of performance of inorganic semiconductor technologies (silicon is still the best at many things it does) but to benefit from a unique set of characteristics combining the electrical properties of (semi)conductors with the properties typical of plastics, that is low cost, versatility of chemical synthesis, ease of processing, and flexibility. Interest in conjugated polymers picked up significantly after the 1976 discovery that they can be made highly electrically conducting following a redox chemical treatment (Chiang *et al.*, 1977). This discovery led to the 2000 Nobel Prize in Chemistry awarded to Alan Heeger, Alan MacDiarmid, and Hideki Shirakawa. By the mid-eighties, many research teams both in academia and industry were investigating  $\pi$ -conjugated oligomers and polymers for their non-linear optical properties or their semiconducting properties, paving the way to the emergence of the fields of plastic electronics and photonics (see, for example, Skotheim, Reynolds and Elsenbaumer, 1997).

The technological developments in plastic electronics and photonics have required to gain a much better fundamental understanding of the nature of electronic excitations, charge carriers, and transport phenomena in ordered and disordered  $\pi$ -conjugated materials. Our aim here is to review some of these issues and to highlight the fascinating chemistry and physics of these materials and the strong connection there exists in this field between basic and applied research.

A major breakthrough in the field of organic electronics is the report by Tang and VanSlyke (1987) at Kodak of the first electroluminescent device based on a  $\pi$ -conjugated molecular material, tris(8-hydroxy-quinoline) aluminium ( $\text{Alq}_3$ ). Shortly thereafter, Friend and his group at Cambridge discovered electroluminescence in a  $\pi$ -conjugated polymer, poly(para-phenylenevinylene), thereby opening the way for the fabrication of polymer light-emitting diodes [LEDs] (Burroughes *et al.*, 1990).

Typically, an organic LED is built (Friend *et al.*, 1999) by depositing successively on a transparent substrate: a transparent electrode made of a high workfunction metal, usually indium-tin oxide (ITO); one or several organic layers that in the case of molecular materials are generally deposited by vacuum sublimation (Sheats *et al.*, 1996) or in the case of polymers by spin-coating or ink-jet printing (Sirringhaus, Kawase, and Friend, 2000); and a top metallic electrode made of a low workfunction metal or alloy. Four main steps are required to generate light from a LED device polarized in forward bias, as sketched on top of Figure 1: (i) *charge injection*: electrons [holes] are injected from the Fermi level of the low [high] workfunction metal into the lowest unoccupied [highest occupied] electronic levels of the organic material present at the metal-organic interface; (ii) *charge transport*: electrons and holes drift in opposite directions within the organic layer(s) under the influence of the static electric field generated by the forward polarization; (iii) *charge recombination*: electrons and holes approaching one another can capture and recombine to lead to the formation of either singlet or triplet excitons; during their lifetime, excitons can hop among molecules/chains via energy-transfer processes; and (iv) *excitation decay*: when excitons decay radiatively, the generated light can escape from the device through the transparent side.

In electrophosphorescent diodes, a phosphorescent dye is present as guest in a host matrix and exciton transfer can take place from the host matrix to the guest; high efficiencies are reached since both singlet and triplet excitations generated in the host can transfer to the guest and contribute to the luminescence signal (Baldo, Thompson, and Forrest, 2000). In conjugated polymer LEDs, only singlet excitons

\*School of Chemistry and Biochemistry, Georgia Institute of Technology, Atlanta, Georgia 30332-0400 and University of Mons-Hainaut, Laboratory for Chemistry of Novel Materials, Place du Parc 20, B-7000 Mons, Belgium.

El director de la revista agradece a Vicente Talanquer las gestiones para conseguir este artículo de Brédas *et al.*

generate light. Organic light-emitting diodes have recently entered the market place as active elements in low-resolution displays such as those commercialized for instance by Pioneer in car stereo systems, by Kodak in digital cameras, or by Philips in electric shavers (Grant, Nolan, and Pinner, 2002). The production of high-resolution full-color flexible displays for televisions is the next target.

Organic materials are also emerging as promising candidates for the fabrication of transistors, photodiodes and solar cells, and (bio)chemical sensors (Horowitz, 1998; Huitema *et al.*, 2002; Halls *et al.*, 1995; Brabec, Sariciftci, and Hummelen, 2001; Zhou, and Swager, 1995; McQuade, Pullen, and Swager, 2000; McQuade, Hegedus and Swager, 2000). In organic field-effect transistors, the key steps are: (i) formation of a conducting channel within the organic semiconductor due to application of a gate voltage; (ii) *charge injection* from the source electrode into the organic semiconductor; (iii) *charge transport* across the organic layer; and (iv) *charge collection* at the drain electrode. Charge injection and collection processes actually correspond to redox reactions, that is electron-transfer reactions.

This brief description highlights the importance of electron-transfer and energy-transfer processes into or within the  $\pi$ -conjugated materials. Thus, the design of new materials with optimal performance requires a fundamental understanding of these processes.

## II. Basic Description of Electron and Energy Transfer

It is useful to point out that both electron-transfer and energy-transfer processes are driven by similar electron-electron and electron-vibration interactions. As a result, they can be described by similar mathematical formalisms, a fact especially clear in the case of weak electronic interactions. Both processes can be viewed as special cases of the non-radiative decay of an electronic state. In the framework of perturbation theory (Balzani, 2001; Bixon, and Jortner, 1999), the probability for a transition from a discrete initial state  $\psi_i$  (corresponding to the reactants) to a discrete final state  $\psi_f$  (corresponding to the products of the reaction) writes under application of a perturbation  $V$  to first order:

$$P_{if} = \frac{1}{\hbar^2} \left| \langle \psi_i | V | \psi_f \rangle \right|^2 \left[ \frac{\sin(\omega_{fi} t / 2)}{\omega_{fi} / 2} \right]^2 \quad (1)$$

where  $t$  denotes time,  $\hbar\omega_{fi}$  the transition energy between the electronic states  $i$  and  $f$  and  $\langle \psi_i | V | \psi_f \rangle$  is the corresponding electronic coupling matrix element. To account for a continuous distribution of final (vibrationally coupled) electronic states, Eq. 1 can be recast by introducing the density of

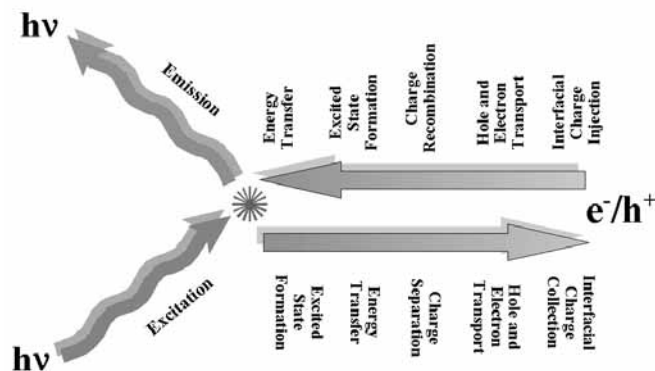


**Figure 1.** Illustration of the various processes governing the operation of (top) organic light-emitting diodes and (bottom) solar cells (adapted from an original sketch by N.R. Armstrong).

final states,  $\rho(E_f)$ , and summing over all probability densities. Assuming that the function  $|\langle \psi_i | V | \psi_f \rangle|^2 \rho(E_f)$  varies slowly with energy, the transition probability per unit time (or transition rate) adopts, in the long-time limit, the simple and widely exploited Fermi's Golden Rule form:

$$k_{if} = \frac{2\pi}{\hbar} \left| \langle \psi_i | V | \psi_f \rangle \right|^2 \rho(E_f) \quad (2)$$

In both electron- and energy-transfer cases, the transition mechanism involves vibrational motions driving the reaction coordinates from reactants to products. The expression for the rate obtained within the Frank-Condon approximation factorizes into an electronic and a vibrational contribution as:

$$k_{if} = \frac{2\pi}{\hbar} |V_{if}|^2 (\text{FCWD}) \quad (3)$$

Here,  $V_{if} = \langle \psi_i | V | \psi_f \rangle$  is the electronic coupling matrix element and (FCWD) denotes the Franck-Condon-weighted density of states. In the high-temperature regime, *i.e.*, when assuming that all vibrational modes are classical ( $\hbar\omega_i \ll k_B T$ ), the FCWD obeys a standard Arrhenius-type equation:

$$(\text{FCWD}) = \frac{1}{\sqrt{4\pi k_B T \lambda}} \exp \left[ -\frac{(\Delta G^0 + \lambda)^2}{4\lambda k_B T} \right] \quad (4)$$

and the rate takes its semiclassical Marcus theory expression (Marcus, 1956; Marcus, 1993; Marcus and Sutin, 1985):

$$k_{if} = \frac{2\pi}{\hbar} |V_{if}|^2 \frac{1}{\sqrt{4\pi k_B T \lambda}} \exp \frac{-(\Delta G^0 + \lambda)^2}{4\lambda k_B T} \quad (5)$$

where  $\lambda$  denotes the reorganization energy induced by the electron or energy transfer and  $\Delta G^0$  is the variation of the Gibbs free energy during the reaction. When the reorganization energy  $\lambda$  is cast into contributions of both classical modes for the surrounding medium [ $(\lambda_0)$ ;  $\hbar\omega_i \ll k_B T$ ] and intramolecular high-frequency vibrational modes [ $(\lambda_i)$ ;  $\hbar\omega_i \gg k_B T$ ], the rate  $k_{if}$  becomes in the context of the Bixon and Jortner (1999) model (for details, see the review in that reference):

$$k_{if} = \frac{2\pi}{\hbar} |V_{if}|^2 \sqrt{\frac{1}{4\pi\lambda_0 k_B T}} \sum_{n=0}^{\infty} \exp(-S_i) \frac{S_i^n}{n!} \exp\left[-\frac{(\Delta G^0 + \lambda_0 + n\hbar\omega_i)^2}{4\lambda_0 k_B T}\right] \quad (6)$$

Here, a single effective quantum mode  $\omega_i$  is assumed to contribute to  $\lambda_i$ . The Huang-Rhys factor,  $S_i = \lambda_i / \hbar\omega_i$ , is a measure of the electron-vibrational coupling interaction. The main effect of high-frequency modes is to renormalize the electronic coupling parameter rather than to contribute to the temperature dependence (except at high temperatures). This discussion underlines that, in order to achieve a complete understanding of the electron or energy transfer properties, a detailed knowledge of the vibrational modes coupled to the transfer process and of the electron-vibration constants is required.

In the next two Sections, we review some recent work that addresses *at the molecular level* the nature of the main parameters that govern electron-transfer processes in  $\pi$ -conjugated oligomers and polymers. We have chosen to focus on oligoacenes since these oligomers are of high current interest. We note that the molecular approach outlined here contrasts with many models developed earlier for organic materials where these processes have been described on a phenomenological basis and from a macroscopic perspective, thereby masking the actual chemical structures of the systems behind effective parameters.

### III. Electron-Vibration Coupling and Reorganization Energy

As emphasized in the previous Section, the reorganization energy is one of the key quantities that control the rates for electron or energy transfer. From the rate expression given in Eq. 6, it is clear that the lower the reorganization energy, the higher the rate.

The reorganization energy is usually expressed as the

sum of inner and outer contributions. The inner (intra-molecular) reorganization energy arises from the change in equilibrium geometry of the donor (D) and acceptor (A) sites consecutive to the gain or loss of electronic charge upon electron transfer (ET). The outer reorganization energy is due to the electronic and nuclear polarization/relaxation of the surrounding medium. It is important to note that, due to the weakness of the van der Waals interactions among organic molecules, the separation of the reorganization energy into inter- and intra-molecular contributions remains largely valid even in the case of molecular crystals. Here, we focus on the intra-molecular reorganization energy in oligoacenes.

In order to illustrate the physical meaning of the intra-molecular reorganization energy, we have represented in Figure 2 the potential energy surfaces (PES) of the donor and acceptor involved in an intermolecular ET reaction of the type  $D + A^+ \rightarrow D^+ + A$ ; in the Figure, the electronic states D1 [A1]

and D2 [A2] correspond to the neutral and cation state of the donor [acceptor], respectively. The ET process can be formally divided into two steps: step *i* is the simultaneous oxidation of D and reduction of  $A^+$  at frozen reactant geometries (in Figure 2, this step corresponds to a vertical transition from the minimum of the D1 surface to D2 and a similar A2 to A1 transition); and step *ii* corresponds to the relaxation of the product nuclear geometries.

As seen from Figure 2, the overall intra-molecular reorganization energy upon electron transfer consists of two terms (Balzani, 2001; Bixon, and Jortner, 1999; Marcus, 1956; Marcus, 1993; Marcus and Sutin, 1985; Reimers, 2001; Silinsh, 1995; Pope, and Swenberg, 1999; Malagoli, and Brédas, 2000; May, and Kühn, 2000):

$$\lambda_i = \lambda_i^{(A^+)} + \lambda_i^{(D^2)} \quad (7)$$

$$\lambda_i^{(A^+)} = E^{(A^+)}(A^+) - E^{(A^+)}(A) \quad (8)$$

$$\lambda_i^{(D^2)} = E^{(D^2)}(D) - E^{(D^2)}(D^+) \quad (9)$$

Here,  $E^{(A^+)}(A^+)$  and  $E^{(A^+)}(A)$  are the energies of the neutral acceptor A at the cation geometry and optimal ground-state geometry, respectively;  $E^{(D^2)}(D)$  and  $E^{(D^2)}(D^+)$  are accordingly the energies of the radical-cation  $D^+$  at the neutral geometry and optimal cation geometry. Eqs. 7-9 remain valid in the case of an energy-transfer process; the difference is only in the nature of the potential energy surfaces and the meaning of the D1, D2, A1, and A2 states ( $\lambda_i$  then corresponds, for instance, to the Stokes shift parameter [May and Kühn, 2000]).

The vertical transitions involved in Figure 2 and Eqs.7-9

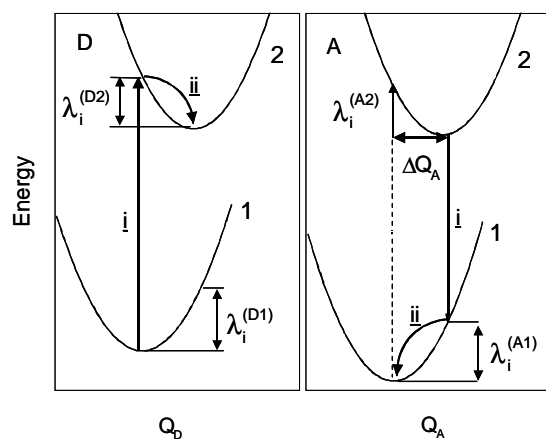


**Figure 2.** Sketch of the potential energy surfaces (in the monomer coordinate representation) related to electron transfer, showing the vertical transitions, the normal mode displacement  $\Delta Q$ , and the relaxation energies  $\lambda_i^{(1)}$  and  $\lambda_i^{(2)}$ .

are consequences of the Franck-Condon principle that requires that the nuclear configurations of the system immediately before and after electron transfer coincide. However, it is important to note that in addition to the Franck-Condon principle, the principle of energy conservation should be also satisfied for electron transfer to occur (Balzani, 2001; Bixon, and Jortner, 1999; Marcus, 1956; Marcus, 1993; Marcus and Sutin, 1985). In the case of optically-driven electron transfer, the mismatch between the electronic vertical transitions (see the lines labeled  $\dot{i}$  in Figure 2) is balanced by the absorption of light. In the case of thermal (dark) electron transfer, in order to satisfy both principles, thermal fluctuations from the equilibrium nuclear configurations of the reactants are needed prior to electron transfer (Marcus, 1956; Marcus, 1993; Marcus and Sutin, 1985).

We have investigated the reorganization energy in oligoacenes containing from 2 to 5 rings: naphthalene, anthracene, tetracene, and pentacene (Gruhn *et al.*, 2002; Coropceanu *et al.*, 2002; Coropceanu *et al.*, 2003; Malagoli *et al.*, 2004; da Silva Filho, submitted; Kwon *et al.*, 2004). These oligomers are of high current interest because of their high charge mobilities in the crystalline state, in particular tetracene, pentacene, and derivatives (Nelson *et al.*, 1998; Sundar *et al.*, 2004). We note that all calculations were performed at the DFT level with the hybrid B3LYP functionals using the standard 6-31G\*\* basis set.

The bond-length modifications upon positive ionization show a consistent trend along the series. Naphthalene displays the largest geometry relaxations, with changes in C–C bond lengths on the order of 0.03 Å. This value is reduced to *ca.* 0.02, 0.015, and 0.01 Å in anthracene, tetracene, and pentacene, respectively. The geometry distortions, as well as

the changes in atomic charge densities (Mulliken populations), are found to spread over the entire molecules. The theoretical estimates of the relaxation energies and total reorganization energies obtained directly from the adiabatic potential energy surfaces are in excellent agreement with the values computed from a normal mode analysis. Our results indicate that the main contribution to the relaxation energy comes from high-energy vibrations. This high-energy contribution is in fact divided over several vibrational modes with wavenumbers in the range 1200–1600  $\text{cm}^{-1}$ . The contribution to  $\lambda_i$  from low-energy vibrations is negligible in anthracene and tetracene and is very small in the case of naphthalene and pentacene.

Gas-phase UPS was used to obtain an experimental estimate of the reorganization energy of anthracene, tetracene, and pentacene (Gruhn *et al.*, 2002; Coropceanu *et al.*, 2002; Coropceanu *et al.*, 2003) (Figure 3). The experimental results confirm that the reorganization process in all three systems is dominated by the interaction with rather high-frequency modes, in agreement with the theoretical results. Overall, the intra-molecular reorganization energies in tetracene (0.11 eV) and pentacene (0.10 eV) rank amongst the smallest  $\lambda_i$  values that have been calculated or measured. They are about three times as small as in TPD (0.29 eV), which is a hole-transport material widely used in organic molecular devices. Interestingly, side-chain derivatizations of pentacene in the form of ethynylsilyl substitutions have been reported by Anthony and co-workers (2001). We have found that such substitutions actually lead to a significant increase in the intra-molecular reorganization energy, by about 50%, due to the involvement of the side-chains in the geometry relaxation process upon ionization. In contrast, Wudl and co-workers have recently synthesized a tetra-methyl derivative of pentacene with the goal of improving the processability of the material (Meng *et al.*, 2003); these authors calculated the reorganization energy in the same way as described above and obtained that it remains exactly the same as in pentacene; the reason is that, in this instance, the substituents have a saturated nature and do not couple to the geometry relaxations of the conjugated backbone.

The origin of the small reorganization energy values in tetracene and pentacene can be traced back to a combination of macrocyclic rigidity and full delocalization of the frontier molecular orbitals (Malagoli *et al.*, 2004; da Silva Filho, submitted; Kwon *et al.*, 2004); the HOMO wavefunctions of anthracene, tetracene, and pentacene are depicted in Figure 3. Accordingly, other molecules that have been found to present small intra-molecular  $\lambda_i$  values are fullerenes, as described by Devos and Lannoo (1998), phthalocyanines (Cornil *et al.*, in press), or discotic macrocycles (Lemaire *et al.*, 2004).

#### IV. Electronic Coupling and Charge Transport

The charge transport properties in conjugated materials critically depend on the packing of the chains and order in the solid state as well as on the density of impurities and structural defects. As a result, the measured mobility values can largely vary as a function of sample quality (Fichou, 2000). Overall, the transport mechanism results from a balance between the energy gained by electron delocalization in an electronic band and the energy gained by geometry relaxation of an individual chain around a charge to form a polaron; the latter term is often referred to as the relaxation (binding) energy of the polaron (Duke and Schein, 1980).

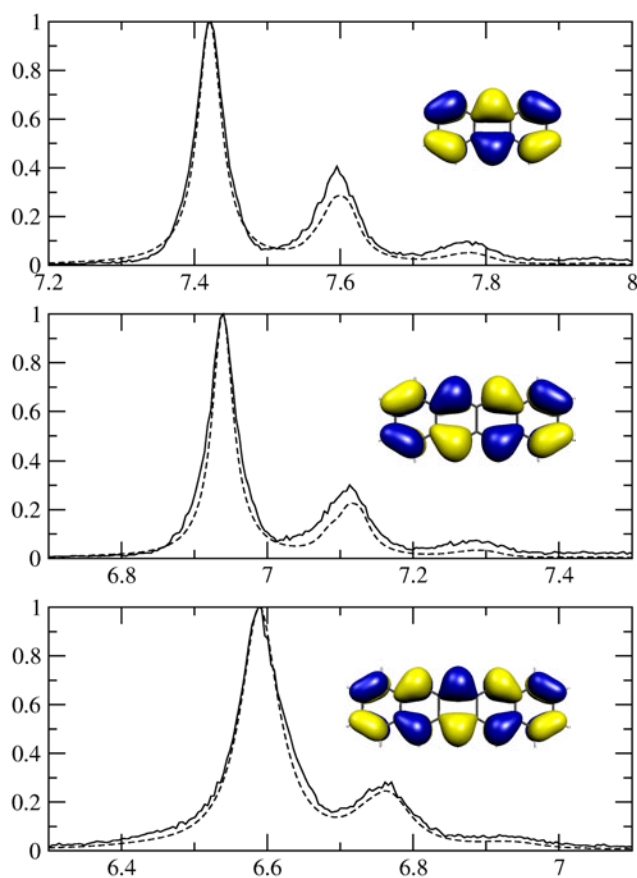


**Figure 3.** DFT/B3LYP simulation (dashed lines) of the vibrational structure of the UPS first ionization peak of anthracene, tetracene, and pentacene (solid lines). The normal modes (8, 7, and 10 modes for anthracene, tetracene, and pentacene, respectively) of the cation species with the largest Huang-Rhys factors have been used for the simulations. A scaling factor of 0.9613 has been applied to the computed frequencies. The transition intensities were convoluted with Lorentzian functions with full-width at half-maximum (FWHM) of 0.046, 0.046, and 0.060 eV for anthracene, tetracene, and pentacene, respectively. The HOMO wavefunctions obtained at the DFT/B3LYP level are also illustrated for each molecule.

In highly purified molecular single crystals such as pentacene, transport at low temperature can be described within a band picture, as shown by Warta, Stehle and Karl (1985). In that case, the positive or negative charge carriers are fully delocalized and their mobilities are a function of the width of the valence or conduction band, respectively, *i.e.*, of the extent of electronic coupling between oligomer chains. In pentacene, low-temperature charge carrier mobilities of up to 60 cm<sup>2</sup>/Vs have been reported (Jurcescu, Baas, and Palstra, 2004). When temperature increases, the mobilities progressively decrease as a result of scattering processes due mainly to lattice phonons, as is the case in metallic conductors. Transport can then be described on the basis of effective bandwidths that are smaller than the bandwidths obtained for a rigid lattice. At an elevated temperature, transport operates via a thermally-assisted polaron hopping regime where localized charge carriers jump between adjacent chains, as shown for instance by Wu and Conwell (1997). As a general rule of thumb, (effective) bandwidths of at least 0.1 eV are needed to stabilize a band regime (Duke and Schein, 1980).

The hopping regime generally implies the presence of significant static disorder, dynamic fluctuations, and/or impurities. For instance, it is expected to operate in spin-coated or ink-jet printed thin films used in polymer devices or in liquid crystalline materials (Brédas *et al.*, 2002; Cornil *et al.*, 2001). At the microscopic level, polaron hopping can be viewed as a self-exchange electron-transfer reaction where a charge hops from an ionized oligomer to an adjacent neutral oligomer, as described in the Introduction, see Eqs. 5 and 6 with  $\Delta G^\circ = 0$ . In that context, the carrier mobilities are a direct function of the electron-transfer rates that, as was described above, are determined by two major parameters: (i) the electronic coupling  $V_{ij}$  between adjacent chains, which needs to be maximized; in the present context, the electronic coupling is often assimilated to the transfer integral,  $t$ , between adjacent chains; and (ii) the reorganization energy  $\lambda$ , which needs to be minimized. As we described several aspects related to reorganization energy in the previous Section, here, we turn most of our attention to the characteristics of the electronic coupling between adjacent  $\pi$ -conjugated chains.

A number of computational techniques, based on *ab initio* or semiempirical methodologies, have been developed to estimate the electronic coupling  $V_{ij}$ ; they have recently been reviewed (Balzani, 2001; Bixon, and Jortner, 1999; Newton, 1991). A robust approach to compute  $V_{ij}$  is to describe the diabatic states of the reactants and products by means of a Slater determinant and to compute their splitting at the transition state (Li, Tang and He, 1999); this approach has been applied by He and co-workers to benzene and biphenyl

dimers using concerted linear reaction coordinates to define the geometry of the transition state (Li and He, 1999). Another approach is to use Koopmans' theorem and to estimate (in the context of a one-electron picture) the transfer integrals  $t$  for holes [electrons] as half the splitting of the HOMO [LUMO] levels in a system made of two chains in the neutral state. In the case of benzene and biphenyl dimers, a good quantitative agreement is observed between the two approaches (except in the strongly interacting regime, not considered here, expected to take place in the case of small molecules separated by short intermolecular distances [Li, Tang and He, 1999; Li and He, 1999]).

The electronic splittings reported below have been calculated within Koopmans' theorem using the semiempirical Hartree-Fock INDO (Intermediate Neglect of Differential Overlap) method; interestingly, the INDO method typically provides transfer integrals of the same order of magnitude as those obtained with DFT-based approaches (Lemaire *et al.*, 2004; Mattheus, 2002). It is of interest to note that when building (infinite) one-dimensional stacks of chains, the widths of the corresponding valence and conduction bands are usually found to be (nearly) equal to four times their respective  $t$  integrals; this indicates that in most instances the tight-binding approximation is relevant. Below, we first discuss transfer integrals in model systems before dealing with the oligoacene crystalline structures.

### Model systems

A first insight into what impacts intermolecular/interchain transfer integrals can be obtained by taking the simple case of a system made of two polyene chains exactly superimposed on top of one another, that is in a cofacial configuration (Brédas *et al.*, 2002; Cornil *et al.*, 2001). Figure 4a illustrates the evolution of the electronic splitting associated to the HOMO and LUMO levels as a function of the number of double bonds along the conjugated backbone. It is observed that: (i) the HOMO splitting is systematically larger than the LUMO splitting; and (ii) the HOMO splitting decreases with chain length while the LUMO splitting displays the opposite behavior

These observations can be rationalized by first looking at the nature of the frontier electronic levels for two ethylene molecules in a cofacial configuration, see Figure 4b. In the isolated ethylene molecule, the HOMO level displays a fully bonding pattern where the lobes of the same sign of the two  $\pi$ -atomic orbitals overlap, while the LUMO level corresponds to the antibonding situation where lobes of opposite sign overlap (thereby introducing a node in the electronic wavefunction in the middle of the bond). When the two molecules interact, the HOMO and LUMO each split into two levels. The magnitude of the HOMO splitting is very

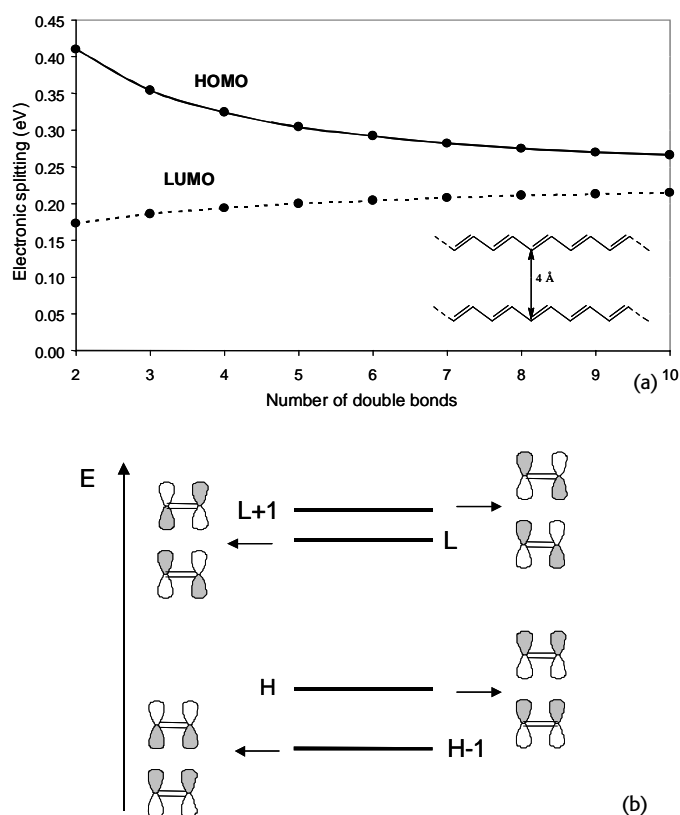


**Figure 4.** a) INDO evolution of the HOMO and LUMO splittings in cofacial systems made of two polyene chains separated by 4 Å as a function of the number of double bonds along the conjugated path; b) illustration of the bonding versus antibonding intermolecular interactions between the HOMO [LUMO] levels of two ethylene molecules in a cofacial configuration.

large, 0.54 eV for an intermolecular distance of 4 Å; the reason is that the interaction between the two molecules gives rise to interchain overlaps that are fully constructive / bonding for the lower level and destructive / antibonding for the upper level, see Figure 4b. The splitting is much smaller for the LUMO level (0.15 eV) since the antibonding character associated to the LUMO level of the isolated molecule yields a mixing of bonding and antibonding interchain overlaps: there occur “direct” bonding interactions (by direct interactions, we mean those between  $\pi$ -atomic orbitals that are exactly superimposed) that are compensated by “diagonal” antibonding interactions in the lower level; in the upper level, “direct” antibonding interactions are compensated by “diagonal” bonding interactions. Thus, the presence of a node in the LUMO wavefunction is responsible for the smaller electronic splitting. Observation (i) is then understood on the basis that in polyene chains the LUMO wavefunction always has one extra node with respect to the HOMO wavefunction. This conclusion actually holds true for conju-

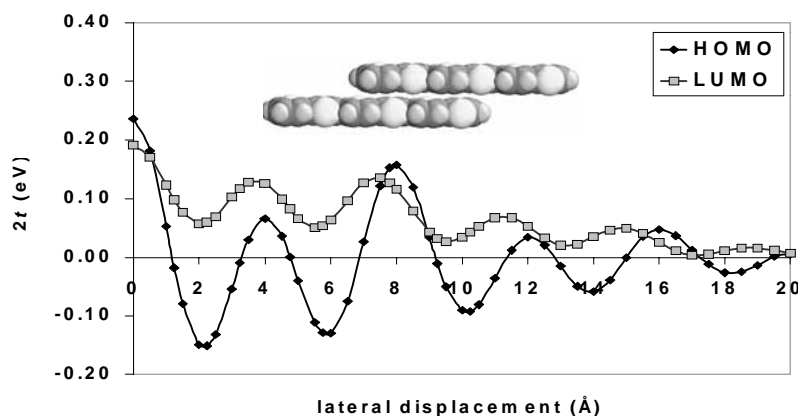


**Figure 5.** INDO evolution of the HOMO and LUMO  $2t$  (splitting) values in a system formed by two sexithienyl chains in a parallel displaced configuration, as a function of the degree of translation of the upper chain.

gated systems with a similar distribution of electronic density in the HOMO and LUMO levels (electron-hole symmetry); this is the case for instance in oligothiophenes, oligophenylene, oligoarylene vinylenes, and their derivatives.

Observation (ii) can be explained by realizing that, in going from ethylene to butadiene, the HOMO [LUMO] level of the isolated butadiene molecule acquires some antibonding [bonding] character; in a cofacially interacting system, this leads to the appearance of “diagonal” antibonding [bonding] interactions, that contribute to decrease [increase] the HOMO [LUMO] splitting. The HOMO and LUMO splittings converge towards the same value for long chains since the impact of a single node difference between the HOMO and LUMO levels attenuates with increasing chain length.

Three important characteristics can be underlined from this simple analysis of perfectly cofacial configurations (Brédas *et al.*, 2002; Cornil *et al.*, 2001): (i) by their very nature, cofacial configurations provide the largest electronic interactions (coupling) between adjacent chains; (ii) as a qualitative rule, the lower the number of nodes in the wavefunction of the frontier level of an isolated chain, the larger the splitting of that level upon cofacial interaction; and (iii) in cofacial stacks of oligomers, the valence bandwidth is expected to be larger for small oligomers and the conduction bandwidth larger for long oligomers; however, for any oligomer length, the valence bandwidth remains larger than the conduction bandwidth. The latter point is the basic reason why it has generally been considered that organic materials should display higher hole mobilities than electron mobilities.

However, perfectly cofacial configurations are hardly encountered in actual crystalline structures. As soon as we move away from such ideal structures, the situation becomes much more complex (Brédas *et al.*, 2002; Cornil *et al.*, 2001).

As an example, we have examined the influence of the relative positions of two interacting oligomers by translating one of them along its long molecular axis. Figure 5 displays the evolution of the  $2t$  values for the HOMO and LUMO splittings in two interacting sexithienyl chains where the top oligomer is translated along its main chain axis while keeping the molecular planes parallel to one another. Note that providing the  $2t$  values rather than the splittings (the latter correspond to the absolute values of  $2t$ ) allows one to illustrate the sign evolution of the transfer integrals.

Figure 5 illustrates the appearance of strong oscillations in the  $2t$  (splitting) values, with a periodicity that is about twice as small for the HOMO splitting as for the LUMO splitting; it also confirms that the largest electronic splittings are calculated for the fully cofacial configurations. The important consequence of the difference in oscillation periods for the HOMO and the LUMO is that small translations can lead to situations where the electronic splitting becomes larger for the LUMO than for the HOMO. For instance, for a displacement of about 1.5 Å along the long chain axis, the reversal in the relative amplitude of the splittings is very significant: we calculate a LUMO splitting about six times as large as the HOMO splitting (0.12 *vs.* 0.02 eV). In such instances, since the conduction bandwidths in oligomer stacks are larger than the valence bandwidths, electrons can be expected to be intrinsically more mobile than holes (provided the reorganization energies in both cases are similar). Thus, this result contrasts with the conventional wisdom expressed earlier that in crystals or crystalline thin films of  $\pi$ -conjugated chains, hole mobility should always be larger than electron mobility.

The calculated evolutions can once again be rationalized from the shape of the HOMO and LUMO orbitals found in the isolated sexithienyl molecule. In the HOMO level, the distribution of the positive and negative LCAO (Linear Combination of Atomic Orbitals) coefficients shows a change in the sign of the wavefunction every half monomer unit, see Figure 6. This pattern thus leads to maxima in the calculated electronic splittings for degrees of translation corresponding to multiples of half the monomer unit size. In contrast, the minima are calculated for geometries where the double bonds of one oligomer are superimposed over the center of the thiophene rings or the inter-ring bonds of the other chain; in such configurations, the global overlap (and hence the HOMO splitting) is considerably reduced by the compensation of bonding and antibonding interactions between the double bonds of one chain and the two adjacent double

bonds of the other chain. In the LUMO level, there is no change in the sign of the LCAO coefficients along the translation axis. This pattern systematically leads to dominant bonding [antibonding] overlaps in the LUMO [LUMO+1] level of the interacting system, and hence to significant electronic splittings; this explains why the minima do not reach values as low as in the HOMO evolution. Maxima [minima] are observed when the thiophene rings of one chain overlap the thiophene rings [the inter-ring bonds] of the second chain; the oscillation period of the curve is thus twice as large as that calculated for the HOMO splitting. Note that the overall decrease in the HOMO and LUMO splittings for increasing translational shifts simply results from the progressive reduction in the overall extent of spatial overlap between the two oligomers.

This discussion illustrates that the amplitudes of the transfer integrals depend on both the relative positions of the interacting molecules/oligomers and the shape (bonding-antibonding pattern) of their frontier molecular orbitals. Thus, the transfer integral amplitudes can hardly be predicted from a simple examination of molecular packing; this underlines the useful role that quantum chemistry can play by providing a molecular-scale understanding of the charge-transport parameters in conjugated systems.

### Crystalline structures

We now turn to a discussion of oligoacenes and describe their interchain transfer integrals on the basis of their actual crystal packing. The single crystals of oligoacenes (Ponomarev, Filipenko, and Atovmian, 1976; Brock and Dunitz, 1990; Holmes *et al.*, 1999; Matheus *et al.*, 2003) are characterized by a layered structure; within these layers, the molecules pack in a herringbone fashion. At first sight, such a molecular arrangement would be expected to lead to only weak overlap between the electronic wavefunctions of adjacent chains since their molecular planes tend to be nearly perpendicular to one another.

Note that there are two inequivalent molecules (labeled 1 and 2 in Figure 7) within the layers of the single crystals considered here. In the case of tetracene, these two molecules have slightly different geometries; as a result, there exists a difference in the energy of the HOMO and LUMO levels of the inequivalent molecules. This difference has to be accounted for when determining the valence and conduction bandwidths in the crystals (Cheng *et al.*, 2003). For two interacting chains, the effective transfer integrals (that are lower than the apparent values) can be determined in the framework of a tight-binding formalism as:

$$2t' = \sqrt{4t^2 - (E_1 - E_2)^2} \quad (10)$$

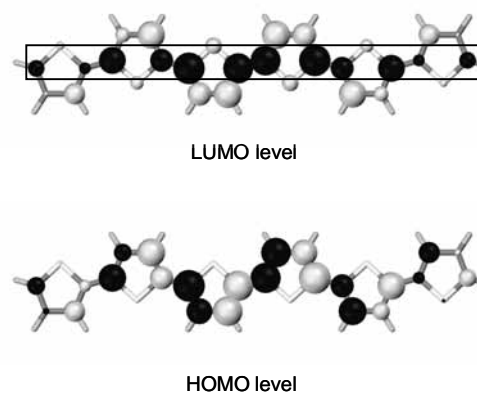


**Figure 6.** Illustration of the LCAO (Linear Combination of Atomic Orbitals) bonding-antibonding pattern of the HOMO (bottom) and LUMO (top) levels in the sexithienyl molecule. The color and size of the circles are representative of the sign and amplitude of the LCAO coefficients, respectively.

where  $t'$  and  $t$  are the effective and apparent interchain transfer integrals, respectively, and  $E_1 - E_2$  denotes the energy offset between the HOMO or LUMO levels of the two chains.

In the oligoacene crystal structures, the transfer integrals between molecules in adjacent layers (*i.e.*, for example along the  $c$  axis in pentacene) are negligible. As a result, charge transport is expected to take place predominantly within the layers, which is in agreement with experiment (Horowitz, 1998; Schoonveld, Vrijmoeth and Klapwijk, 1998). This implies that the achievement of high carrier mobilities in field-effect transistors requires a proper orientation of the layers within the semiconductor channel. In the oligoacene single crystals, significant electronic splittings arise along the axis connecting cofacially-displaced molecules (*i.e.*, the  $a$  axis in the pentacene crystal, see Figure 7) and the diagonal axes  $d$  along the herringbone.

The evaluation of the three-dimensional band-structures of the oligoacene single crystals, based on the INDO-calculated splittings between adjacent chains, leads to very significant bandwidths for both the valence and conduction bands (Cheng *et al.*, 2003). The results indicate that: (i) the electronic splittings are very similar for electrons and holes; (ii) both the HOMO and LUMO splittings increase with molecular size, in contrast to the evolution found in cofacial geometries (*vide supra*); and (iii) the bandwidths are very significant and range from 300 meV in naphthalene to 700 meV in pentacene. This compares very well with the bandwidths obtained at the DFT level for pentacene (Tiago, Northrup, and Louie, 2003); in contrast, the bandwidths obtained with the Extended Hückel formalism are two to three times smaller (Had-don *et al.*, 2002).

These results are consistent with the achievement of a band regime at low temperature in perfectly ordered and purified oligoacene crystals. Importantly, in pentacene, there occurs an interesting combination of large bandwidths with small reorganization energies, as described in the previous Section. This suggests that the band regime could be operative up to relatively high temperatures; very recent measurements on ultra-purified crystals actually show hole mobilities at room temperature as large as  $35 \text{ cm}^2/\text{Vs}$  (Jurchescu, Baas, and Palstra, 2004).

It is worth noting that when the crystal unit cell contains two inequivalent molecules, the valence and conduction bands are actually made of two sub-bands of different widths. The hole [electron] mobility then depends on the curvature of the top [bottom] of the upper [lower] band in the valence [conduction] band, or to first approximation, on the width of these sub-bands. While the widths of the total valence and conduction bands are very similar in the pentacene single crystal (around 730 meV), the upper occupied and lower unoccupied sub-bands are 523 and 183 meV wide, respectively (Cheng *et al.*, 2003). This suggests that in the band regime hole mobility is larger than electron mobility; the same is expected in the hopping regime, since we pointed out at the end of the previous Section that the electron-vibration couplings are larger than the hole-vibration couplings.

Thus, combining the results of calculations on transfer integrals (electronic couplings) and on reorganization energies (electron- and hole-vibration constants) can provide very useful trends regarding the intrinsic electron and hole mobilities in  $\pi$ -conjugated materials. However, much work

remains to be done to be in a position to estimate directly carrier mobilities. In particular, while significant progress has been made towards an accurate determination of the couplings with intramolecular vibrations, improvements are still required with regard to a molecular description of the couplings with lattice vibrations (phonons) and of the medium polarization (electronic relaxation) effects.

## V. Synopsis

The description of the electronic structure of  $\pi$ -conjugated materials has come a long way since the first calculations on polyenes and the attention given to the issues of bond-length alternation and ordering of the lowest singlet excited states. After the discovery of highly conducting polymers, much of the interest focused on the evaluation of the ground-state properties (ionization potential, electron affinity, bandgap, bandwidths) and the evolution of the geometry and optical properties upon ionization (triggering the development of concepts such as solitons, polarons, and bipolarons). In the mid-1980's, with the increased importance attached to non-linear optical properties, the goal of many calculations was to determine the nature of the (unrelaxed) excited states playing a role in the second-order and third-order molecular polarizabilities. Relaxation effects in the excited states and impact of intermolecular interactions became the focus of numerous quantum-chemical studies in the 1990's due to the advent of electroluminescent conjugated polymers.

What we hope to have portrayed in this contribution is the increased significance of the dynamic processes taking place in  $\pi$ -conjugated materials, be them charge transport, charge injection, exciton diffusion, or exciton dissociation (Brédas *et al.*, submitted). As a result, much attention is now devoted to the calculation of the rates for such energy-transfer or electron-transfer reactions, as they impact the characteristics of organic materials to be used in the new generations of electronic and photonic plastic devices.

## Acknowledgements

The work on  $\pi$ -conjugated materials at Georgia Tech is partly supported by the National Science Foundation (through the STC Program under Award Number DMR-0120967, the MRSEC Program under Award Number DMR-0212302, and grant CHE-0342321), the Office of Naval Research, the Georgia Tech "Center on Organic Photonics and Electronics (COPE)", and the IBM Shared University Research Program. The work in Mons is partly supported by the Belgian Federal Government "InterUniversity Attraction Pole in Supramolecular Chemistry and Catalysis (PAI 5/3)" and the Belgian National Fund for Scientific Research (FNRS). JC and DB are FNRS Research Fellows. ■

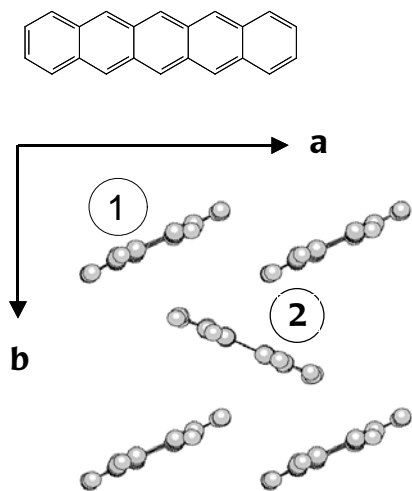


**Figure 7.** Illustration of the crystal packing of pentacene. We display here the layout of the molecules within one layer. Labels 1 and 2 refer to the inequivalent molecules in the unit cell of pentacene.

## References

- Anthony, J.E., Brooks, J.S., Eaton, D.L. and Parkin, S.R., *J. Am. Chem. Soc.*, **123**, 9482, 2001.
- Baldo, M.A., Thompson, M.E., and Forrest, S.R., *Nature* **403**, 750, 2000.
- Balzani, V. (Ed.), *Electron Transfer in Chemistry*, Wiley-VCH, Weinheim, 2001.
- Bixon, M., and Jortner, J. (Eds.), *Electron Transfer: From Isolated Molecules to Biomolecules*, *Adv. Chem. Phys.*, Vols. 106-107, Wiley, New York, 1999.
- Brabec, C.J., Sariciftci, N.S., and Hummelen, J.C., *Adv. Funct. Mater.*, **11**, 15, 2001.
- Brédas, J.L., Calbert, J.P., da Silva Filho, D.A. and Cornil, J., *Proc. Nat. Acad. Sci. USA*, **99**, 5804, 2002
- Brédas, J.L., Beljonne, D., Coropceanu, V. and Cornil, J., *Chem. Rev.*, **104**, 4971, 2004.
- Brock, C.P. and Dunitz, J.D., *Acta Crystallogr. Sect. B: Struct. Sci.*, **46**, 795, 1990.
- Burroughes, J.H., Bradley, D.D.C., Brown, A.R., Marks, R.N., Friend, R.H., Burn, P.L., and Holmes, A.B., *Nature*, **347**, 539, 1990.
- Cheng, Y.C., Silbey, R.S., da Silva Filho, D.A., Calbert, J.P., Cornil, J. and Brédas, J.L., *J. Chem. Phys.*, **118**, 3764, 2003.
- Chiang, C.K., Park, Y.W., Heeger, A.J., Shirakawa, H., Louis, E.J. and MacDiarmid, A.G., *Phys. Rev. Lett.*, **39**, 1098, 1977.
- Cornil, J., Lemaire, V., Steel, M.C., Dupin, H., Burquel, A., Beljonne, D. and Brédas, J.L., in Sun, S. and Sariciftci, N.S., (Eds.), *Organic Photovoltaics: Mechanisms, Materials and Devices*, Marcel Dekker, New York, in press.
- Cornil, J., Beljonne, D., Calbert, J.P. and Brédas, J.L., *Adv. Mater.*, **13**, 1053, 2001.
- Coropceanu, V., Malagoli, M., da Silva Filho, D. A., Gruhn, N. E., Bill, T. G. and Brédas, J. L., *Phys. Rev. Lett.*, **89**, 275503, 2002.
- Coropceanu, V., Andre, J. M., Malagoli, M. and Brédas, J. L., *Theor. Chem. Acc.*, **110**, 59, 2003.
- Da Silva Filho D.A., Friedlein, R., Coropceanu V., Öhrwall, G., Osikowicz, W., Suess, C., Sorensen S.L., Svensson, S., Salaneck W.R. and Brédas, J.L. *Chem. Commun.*, **1702**, 2004.
- Devos, A. and Lannoo, M. *Phys. Rev. B*, **58**, 8236, 1998.
- Duke, C.B. and Schein, L.B., *Physics Today*, p. 42, 1980 (February).
- Fichou, D., *J. Mater. Chem.*, **10**, 571, 2000.
- Friend, R.H., Gymer, R.W., Holmes, A.B., Burroughes, J.H., Marks, R.N., Taliani, C., Bradley, D.D.C., dos Santos, D.A., Brédas, J.L., Lögdlund, M., and Salaneck W.R., *Nature*, **397**, 121, 1999.
- Grant, E., Nolan, P., and Pinner, D., *The McKinsey Quarterly*, **1**, 18, 2002.
- Gruhn, N. E., da Silva Filho, D. A., Bill, T. G., Malagoli, M., Coropceanu, V., Kahn, A. and Brédas, J. L., *J. Am. Chem. Soc.*, **124**, 7918, 2002.
- Haddon, R.C., Chi, X., Itkis, M.E., Anthony, J.E., Eaton, D. L., Siegrist, T., Mattheus, C.C. and Palstra, T.T.M., *J. Phys. Chem., B*, **106**, 8288, 2002.
- Halls, J.J.M., Walsh, C.A., Greenham, N.C., Marseglia, E.A., Friend, R.H., Moratti, S.C., and Holmes, A.B., *Nature*, **376**, 498, 1995.
- Holmes, D., Kumaraswamy, S., Matzger, A.J. and Vollhardt, K.P.C., *Chem. Eur. J.*, **5**, 3399, 1999.
- Horowitz, G., *Adv. Mater.*, **10**, 365, 1998.
- Huitema, H.E.A., Gelinck, G.H., van der Putten, J.B.P.H., Kuijk, K.E., Hart, K.M., Cantatore, E., and de Leeuw, D.M., *Adv. Mater.*, **14**, 1201, 2002.
- Jurchescu, O.D., Baas, T. and Palstra, T.T.M., *Appl. Phys. Lett.*, **84**, 3061, 2004.
- Kwon, O., Coropceanu V., Gruhn, N. E., Durivage, J. C., Laquindanum, J. G., Katz, H. E., Cornil, J. and Brédas, J. L., *J. Chem. Phys.*, **2004**, 120, 8186.
- Lemaire, V., da Silva Filho, D.A., Coropceanu V., Lehmann, M., Geerts, Y., Piris, J., Debije, M.G., van de Craats, A.M., Senthilkumar, K., Siebbeles, L.D.A., Warman, J.M., Brédas, J.L. and Cornil, J., *J. Am. Chem. Soc.*, **126**, 3271, 2004.
- Li, X.Y., and He, F.C., *J. Comput. Chem.*, **20**, 597, 1999.
- Li, X.Y., Tang, X.S. and He, F.C., *Chem. Phys.*, **248**, 137, 1999
- Malagoli, M. and Brédas, J. L., *Chem. Phys. Lett.*, **327**, 13, 2000.
- Malagoli, M., Coropceanu V., da Silva Filho, D.A. and Brédas, J.L., *J. Chem. Phys.*, **120**, 7490, 2004.
- Mattheus, C.C., "Polymorphism and Electronic Properties of Pentacene", Ph.D. Thesis, University of Groningen, The Netherlands, 2002.
- Mattheus, C.C., de Wijs, G.A., de Groot, R.A. and Palstra, T.T.M., *J. Am. Chem. Soc.*, **125**, 6323, 2003
- May, V. and Kühn, O. (Eds.), *Charge and Energy Transfer Dynamics in Molecular Systems* Wiley-VCH, Berlin, 2000.
- Marcus, R.A., *J. Chem. Phys.*, **24**, 966 and 979, 1956.
- Marcus, R.A., *Reviews of Modern Physics* **65**, 599, 1993.
- Marcus, R.A. and Sutin, N., *Biochimica Biophysica Acta*, **811**, 265, 1985.
- McQuade, D.T., Hegedus, A.H. and Swager, T.M., *J. Am. Chem. Soc.* **122**, 12389, 2000.
- McQuade, D.T., Pullen, A.E., and Swager, T.M., *Chem. Rev* **100**, 2537, 2000.
- Meng, H., Bendikov, M., Mitchell, G., Helgeson, R., Wudl, F., Bao, Z., Siegrist, T., Kloc, C. and Chen, C.H., *Adv. Mater.* **15**, 1090, 2003.
- Nelson, S.F., Lin, Y.Y., Gundlach, D.J. and Jackson, T.N., *Appl. Phys. Lett.* **72**, 1854, 1998.
- Newton, M.D., *Chem. Rev.* **91**, 767 1991.
- Ponomarev, V.I., Filipenko, O.S. and Atovmyan, L.O., *Kristallografiya*, **21**, 392, 1976.
- Pope, M. and Swenberg, C. E. (Eds.), *Electronic Processes in Organic Crystals and Polymers*, 2<sup>nd</sup> edition, Oxford University Press, New York, 1999.
- Reimers, J. R., *J. Chem. Phys.* **115**, 9103, 2001.
- Schoonveld, W.A., Vrijmoeth, J. and Klapwijk, T.M., *Appl. Phys. Lett.* **1998**, 73, 3884.
- Sheats, J.R., Antoniadis, H., Hueschen, M., Leonard W., Miller, J., Moon, R., Roitman, D., and Stocking, A., *Science* **273**, 884, 1996.
- Silinsk, E. A., Klimkans, A., Larsson, S. and Capek, V., *Chem. Phys.* **198**, 311, 1995.
- Sirringhaus, H., Kawase, T., and Friend, R.H., *Science*, **290**, 2123, 2000.
- Skotheim, T.A., Reynolds, J.R., and Elsenbaumer, R.L., (Eds.), *Handbook of Conducting Polymers*, 2<sup>nd</sup> Edition, Marcel Dekker, New York, 1997
- Sundar, V.C., Zaumseil, J., Podzorov, V., Menard, E., Willett, R.L., Someya, T., Gershenson, M.E. and Rogers, J.A., *Science*, **303**, 1644, 2004.
- Tang, C.W. and VanSlyke, S.A., *Appl. Phys. Lett.*, **51**, 913, 1987.
- Tiago, M.L., Northrup, J.E. and Louie, S.G., *Phys. Rev., B*, **67**, 115212, 2003.
- Warta, W., Stehle, R. and Karl, N., *Appl. Phys. A*, **36**, 163, 1985.
- Wu, M.W. and Conwell, E.M., *Chem. Phys. Lett.*, **266**, 363, 1997.
- Zhou, Q., and Swager, T.M., *J. Am. Chem. Soc.*, **117**, 12593, 1995.